Spin and orbital magnetism in ordered $Fe_{3\pm\delta}Si_{1\mp\delta}$ binary Heusler structures: Theory versus experiment

Khalil Zakeri,[1,*] S. Javad Hashemifar,[1,2,†] Jürgen Lindner,[1] Igor Barsukov,[1] Ralf Meckenstock,[1] Peter Kratzer,[1,2] Zdeněk Frait,[2] and Michael Farle[1]

[1]*Fachbereich Physik and Center for Nanointegration (CeNIDE), Universität Duisburg-Essen, Lotharstrasse 1, 47048 Duisburg, Germany*

[2]*Institute of Physics, Academy of Sciences of the Czech Republic, Na Slovance, 18221 Prague 8, Czech Republic*

(Received 19 October 2007; published 21 March 2008)

The spin and orbital magnetism of 8 nm thick $Fe_{2.8}Si_{1.2}$, Fe_3Si, and $Fe_{3.2}Si_{0.8}$ films epitaxially grown on MgO(001) was determined experimentally by ferromagnetic resonance and superconducting quantum interference device magnetometry and theoretically by fully relativistic density functional theory calculations. The experimental average spin (orbital) moment of the stoichiometric Fe_3Si [$\mu^{av}_{S(L)}=1.38(0.051)\mu_B$] is in reasonable agreement with the theoretical one [$\mu^{av}_{S(L)}=1.75(0.029)\mu_B$]. Slight increases (reductions) of the Fe content are experimentally found to increase (decrease) the spin and orbital moments as predicted by theory. The results reveal an important step toward tailoring spin and orbital magnetism in the binary Heusler alloys.

DOI: 10.1103/PhysRevB.77.104430 PACS number(s): 85.75.−d, 71.15.Mb, 75.20.Hr, 76.50.+g

I. INTRODUCTION

All magnetic and transport phenomena in novel spintronic materials are directly influenced by the relative orientation of the element specific spin and orbital magnetism making their investigation of major interest in recent years. The orbital moment of 3*d* transition metals and most of their compounds is considerably smaller than the spin moment and strongly modified by the local environment and crystal symmetry. Determination of the orbital moment requires a highly accurate technique. The element selective orbital moment of the Heusler alloys, which has been identified as one of the most interesting class of materials for *spintronics,* has been investigated experimentally (using x-ray magnetic circular dichroism)[1–7] and theoretically.[8–10] An enhanced orbital moment was observed in some experiments[1–3] which could not be explained theoretically and might have been caused by residual oxidation of the 3*d* element.

Fe_3Si is a binary Heusler alloy with well-ordered $D0_3$ structure and can be epitaxially grown using the molecular beam epitaxy technique.[11–17] As the ratio of the orbital to the spin moment μ^{av}_L/μ^{av}_S of Fe_3Si is small, the Kittel formula[18] which is valid only for $\mu^{av}_L/\mu^{av}_S \ll 1$ can be used to extract the orbital to the spin moment ratio from the measured *g* factor in a ferromagnetic resonance (FMR) experiment.[18] The possibility of epitaxial growth of Fe_3Si and the applicability of the Kittel formula in this compound make it an appropriate prototype system for the orbital moment investigation of binary Heusler alloys.

In this paper we report the experimental results of the average spin and orbital magnetism of $Fe_{3\pm\delta}Si_{1\mp\delta}$ binary Heusler structures probed by a combination of FMR and superconducting quantum interference device (SQUID) magnetometry. Moreover, to identify the role of the type and the configuration of nearest neighbors on the average moments, the electronic structure and the local magnetic moments of FeSi, Fe_3Si, and Fe are calculated within the framework of the density functional theory (DFT). We find that the average values of both spin and orbital magnetism in this binary Heusler structure are smaller than the corresponding values of Fe bulk. It will be demonstrated that both spin and orbital moments are tunable by slightly changing the Fe concentration.

II. EXPERIMENTAL DETAILS

The 8 nm thick epitaxial $Fe_{3\pm\delta}Si_{1\mp\delta}$ ($\delta=0$ and 0.2) films were grown on MgO(001) in a molecular beam epitaxy system with a base pressure of 1×10^{-9} mbar. The MgO(001) substrate was first cleaned by isopropanol in an ultrasonic bath, afterward transferred into an ultrahigh vacuum (UHV) chamber. Inside the UHV chamber, the substrate was annealed at 1200 K for 30 min. The films were grown by coevaporation of ^{57}Fe and Si at a substrate temperature $T_s=485$ K and a growth rate of about 1 nm/min, which was monitored by a calibrated quartz microbalance. In order to obtain the well-ordered $D0_3$ structure, the samples were annealed immediately after deposition in UHV at $T_a=900$ K for 1 h and finally were capped with 5 nm of chromium to avoid any oxidation. The structure and stoichometry of the samples were examined by x-ray diffraction and energy dispersive x-ray analysis (for more details, see Ref. 19).

The FMR experiments were performed between 1 and 70 GHz (at 26 different microwave frequencies) in order to precisely determine the *g* factor and consequently the ratio of orbital to spin moment. The sample's magnetization was quantitatively determined by measuring the SQUID hysteresis loops.

III. THEORETICAL ASPECTS

The theoretical results were obtained using full relativistic DFT calculations. The WIEN2K computational package[20] that uses the full-potential linear augmented plane wave (FP-LAPW) method to solve the single-particle Kohn-Sham equations was employed. In the FP-LAPW method, the unit cell is partitioned into two regions, nonoverlapping spheres around the nucleus (muffin-tin spheres) and the remaining interstitial region. In the muffin-tin spheres, the wave function is expanded into the atomic orbitals and lattice harmonics, while in the interstitial region, plane waves are used as

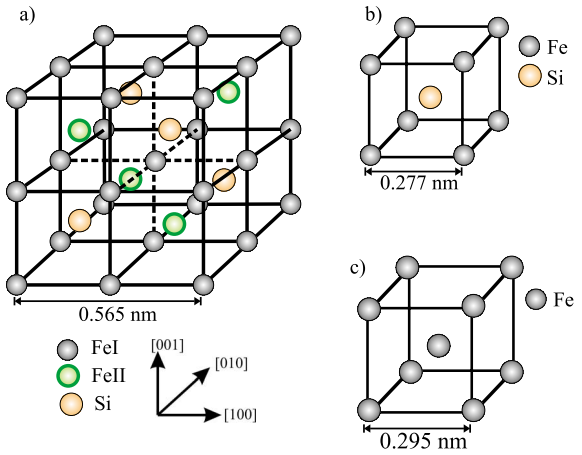

FIG. 1. (Color online) Schematic representation of (a) $D0_3$ structure of Fe_3Si, (b) $B2$ structure of FeSi, and (c) bcc structure of Fe. The $D0_3$ structure consists of four bcc and four $B2$ sublattices.

the basis set. The exchange-correlation energy was calculated by using the generalized gradient approximation (GGA).[21] The relativistic spin-orbit correction and orbital polarization were taken into account, which enable us to determine the orbital contributions to the magnetic moments. The orbital polarization parameter was calculated independently by an *ab initio* method. In our calculations, we consider a lattice parameter of $a=0.565$ nm [obtained by our x-ray diffraction (XRD) measurements], cutoff energy of $E_{\text{cut}}=14.51$ Ry, and k points of $10\times10\times10$.

IV. RESULTS AND DISCUSSION

As it is shown in Fig. 1(a), there are two different Fe atoms in the unit cell of the $D0_3$ lattice, and we found that the local moment on Fe II sites is significantly larger than the one on Fe I sites, in good agreement with previous theoretical[22–26] and experimental[16,27] investigations. The calculation shows that Fe atoms at Fe I sites have a spin (orbital) moment of $\mu_S=1.35$ $(\mu_L=0.022)\mu_B$ and at Fe II sites, $\mu_S=2.57$ $(\mu_L=0.042)\mu_B$. The spin moment of Si was found to be very small and oppositely oriented to the one of Fe $(\mu_S=-0.067\mu_B)$. Its orbital moment was practically zero, hence both contributions to the average total moment of the unit cell $(\mu_{\text{tot}}^{\text{theo}}=5.2\mu_B)$ can be neglected. In order to calculate the average spin (orbital) moment of Fe, we assume a Russel-Saunders (L-S)-type coupling[28] where the average spin (orbital) moment of Fe atoms in $D0_3$ structure of Fe_3Si can be expressed as $\mu_{S(L)}^{\text{av}}=(8\mu_{S(L),\text{Fe I}}+4\mu_{S(L),\text{Fe II}})/(8\text{ Fe I}+4\text{ Fe II})$. Here, the denominator represents the total number of Fe atoms in the unit cell, which are 8 Fe I plus 4 Fe II atoms. This approach leads to an average spin and orbital moment of $\mu_S^{\text{av}}=1.73\mu_B$ and $\mu_L^{\text{av}}=0.029\mu_B$. Moreover, our calculations show that Fe_3Si has metallic character which has also been predicted by other groups.[22–26]

The total magnetic moment of the unit cell for our binary Heusler alloy is a noninteger number, while for most full Heusler alloys, it is an integer number. One should note, however, that this property of the magnetic moment is not a universal law valid for Heusler alloys.[8]

TABLE I. The calculated (upper part) g factor, average spin, and orbital moments of FeSi, Fe_3Si, and Fe in comparison to the experimental ones of 8 nm $Fe_{2.8}Si_{1.2}$, Fe_3Si, and $Fe_{3.2}Si_{0.8}$ thin films (lower part). The error bars in μ_S^{av} and μ_L^{av} are less than 6% and mainly result from the uncertainty of the sample volume.

System	g factor	μ_S^{av} [μ_B/atom]	μ_L^{av} [10^{-3} μ_B/atom]
		Theory	
FeSi	2.002	0.00	0.0
Fe_3Si	2.035	1.75	29
Fe	2.069	2.28	76
		Expt	
$Fe_{2.8}Si_{1.2}$	2.067	1.32	45
Fe_3Si	2.075	1.38	51
$Fe_{3.2}Si_{0.8}$	2.085	1.53	65
Fe	2.092	2.24	103

For transition metals, it is rather common that the local-density approximaton (LDA)/GGA severely underestimates the orbital moment. For instance, for bcc Fe, LDA finds a value of $\mu_L\approx0.04\mu_B$ instead of the experimental value of $\mu_L\approx0.1\mu_B$.[29] In principle, a precise calculation of the orbital moment requires the consideration of an *orbital dependent orbital polarization*. Although the LDA/GGA + orbital polarization gives better values[30] and was taken into account in our calculations, the calculated values are small and cannot be directly compared to the measured ones. However, the relative changes with respect to the value of the Fe bulk are in acceptable agreement with experiment and help us to better understand our results.

In order to shed light onto the origin of the quenching of orbital moments in Fe_3Si and to distinguish the contribution of the site specific magnetic moments to the average moment, the spin and orbital moments were calculated for two additional cases: (i) bcc Fe and (ii) FeSi ordered in $B2$ structure [a schematic drawing of the structures is shown in Figs. 1(b) and 1(c), respectively], using the same theoretical approach mentioned above. The calculated spin and orbital moments are listed in the upper part of Table I.

The calculations indicate that μ_S^{av} and μ_L^{av} of Fe atoms in the Fe_3Si compound are considerably smaller than the corresponding values in bcc Fe (see Table I). The reduction of the spin and orbital moments in Fe_3Si alloy, compared to the Fe bulk, can be attributed to the Fe-Si bonding and hybridization that change the Fe band structure near the Fermi level (see below). Based on the calculated moments in FeSi, we conclude that increasing the Si concentration to 50% completely quenches the ferromagnetic character of the system.

Orbital quenching is a well-known phenomenon in $3d$ ferromagnetic transition metals (Fe, Co, and Ni), which is caused by the strong ligand field of these materials lifting the degeneracy of the angular momentum. Increasing the Si concentration increases the ligand field strength and consequently enhances the orbital quenching effects on Fe atoms. This extreme quenching was observed in the calculation for the $B2$ structure of FeSi in which every Fe atom is surrounded by eight nearest Si neighbors. This geometry indi-

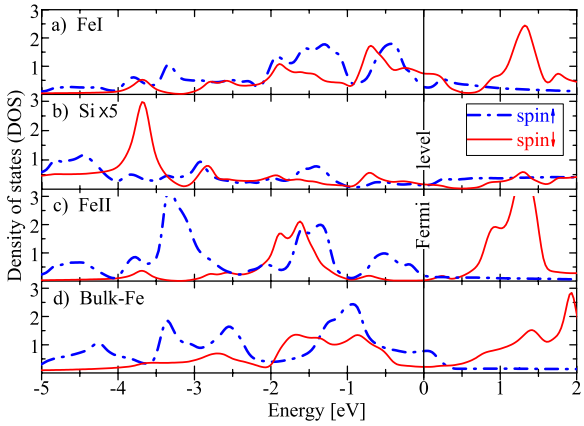

FIG. 2. (Color online) Calculated spin resolved DOS of the (a) Fe I, (b) Si, (c) Fe II atoms in Fe_3Si lattice, and (d) bulk Fe. The solid curves represent the minority spins, whereas the dashed-dotted curves represent the majority ones.

cates a strong Fe-Si hybridization in this system that leads to a complete quenching of the moments.

A perfect $D0_3$ lattice of Fe_3Si consists of 4 bcc and 4 $B2$ sublattices [12 Fe atoms, 8 Fe I, 4 Fe II, and 4 Si atoms (see Fig. 1)]. The first argument for a direct effect of Fe-Si hybridization on orbital quenching is based on the difference in the density of states (DOS) of Fe I and Fe II atoms in ordered Fe_3Si alloy resulting from our calculations. Fe II in this alloy has eight Fe nearest neighbor, whereas Fe I has four Fe and four Si nearest neighbor. Hence, Fe I has more effective hybridization with Si and consequently a smaller magnetic moment compared to Fe II. In Fig. 2, the spin resolved DOS of Fe_3Si projected onto atomic species is compared to the corresponding DOS in bulk Fe. It is observed that the minority states of Fe I (i) are enhanced with respect to the bulk Fe and (ii) very similar to the minority states of Si. The DOS in Fe I (in particular, minority spin states) is very different from the one of Fe bulk which, in turn, explains the small spin moment. The similarity of the minority spins of Fe I d states and Si p states is another direct evidence of the hybridization explaining the quenched orbital moment via the enhanced ligand field effects on the Fe I atoms.

The absolute value of μ_S^{av} and μ_L^{av} can be determined by measurements of the g factor and the total magnetization by SQUID magnetometry. In principle, g is a tensor whose elements can be determined by performing a frequency-dependent measurement along different crystallographic directions. Assuming principle crystallographic directions for the external magnetic field, the frequency dependence of the FMR resonance field can be simplified as follows:

$$B \parallel \langle 100\rangle: \left(\frac{\omega}{\gamma_\parallel}\right)^2 = \left(B_{\mathrm{res}\parallel} + \frac{2K_4}{M}\right)\left(B_{\mathrm{res}\parallel} - \mu_0 M_{\mathrm{eff}} + \frac{2K_4}{M}\right), \tag{1}$$

$$B \parallel \langle 110\rangle: \left(\frac{\omega}{\gamma_\parallel}\right)^2 = \left(B_{\mathrm{res}\parallel} - \frac{2K_4}{M}\right)\left(B_{\mathrm{res}\parallel} - \mu_0 M_{\mathrm{eff}} + \frac{K_4}{M}\right), \tag{2}$$

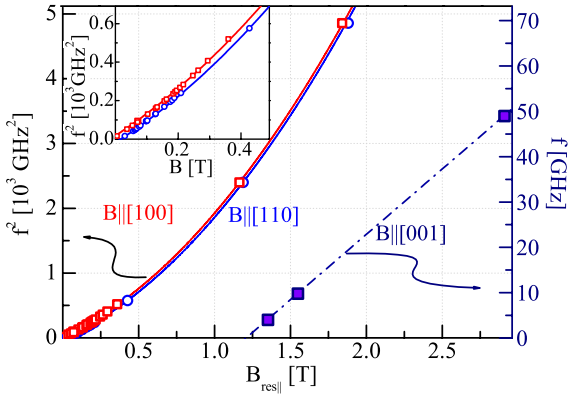

FIG. 3. (Color online) The resonance frequency squared versus the resonance field for magnetic fields applied parallel to the [100] (open squares) and [110] (open circles) directions (left axis). The solid squares denote the resonance field dependence of the resonance frequency (right axis) for an external magnetic field along the film normal ([001] direction). The solid curves and the dashed-dotted line are fits according to Eq. (1)–(3) yielding an isotropic g factor of 2.075(5). The inset shows the low frequency results.

$$B \parallel [001]: \frac{\omega}{\gamma_\perp} = B_{\mathrm{res}\perp} + \mu_0 M_{\mathrm{eff}} + \frac{2K_4}{M}, \tag{3}$$

where K_4 is the cubic magnetic anistropy energy (MAE) constant and $\mu_0 M_{\mathrm{eff}}$ denotes the effective perpendicular anisotropy field which is related to the perpendicular MAE $K_{2\perp}$, and magnetization M, according to $\mu_0 M_{\mathrm{eff}} = (2K_{2\perp}/M - \mu_0 M)$. Equations (1) and (2) indicate that for the in-plane configuration (the external magnetic field applied in the film plane), frequency squared versus resonance field B_{res} is a parabolic function, whereas in the out-of-plane configuration (the external magnetic field applied along the film normal), the frequency dependence of the resonance field is linear [Eq. (3), for more details see, for example, Refs. 31 and 32].

Our angle-dependent FMR measurements show that the samples exhibit rather small values of the magnetic parameters compared to bulk Fe. The cubic anisotropy field of the stoichiometric Fe_3Si $K_4/M = 4.5(1)$ mT is much smaller than the corresponding value of bulk Fe $K_4/M = 28(1)$ mT (for more details, see Ref. 19). Furthermore, the analysis of the FMR linewidth which provides information on magnetic relaxation processes shows that in addition to the Gilbert mechanism, two-magnon scattering plays an important role in the relaxation mechanism. A detailed determination of the magnetic relaxation parameters can be found elsewhere.[33]

The g factor measured by FMR provides an access to the ratio of the orbital to the spin moment according to the Kittel formula:[18,31,34–36] $g = g_{\mathrm{electron}} + 2(\mu_L^{\mathrm{av}}/\mu_S^{\mathrm{av}})$; $g_{\mathrm{electron}} = 2.002\,319$.

In Fig. 3, the FMR results for a stoichiometric sample are shown. The parabolic behavior for the in-plane geometry according to Eqs. (1) and (2) is observed and the analysis yields a g factor of 2.075(5). The analysis for the perpendicular configuration yields the same g factor showing that it is isotropic. With Kittel's formula, one obtains $\mu_L^{\mathrm{av}}/\mu_S^{\mathrm{av}} = 0.037(3)$. From SQUID measurements, we find M

$=879$ kA/m for the total magnetic moment per volume that is a sum of the spin and orbital moments of all atoms ($\mu_S^{av}+\mu_L^{av}$). This results in a total moment of the unit cell of $\mu_{total}^{expt}=4.2\mu_B$. By combining the SQUID and FMR results and assuming a *L*-*S* type of coupling, we obtain $\mu_S^{av}=1.38\mu_B$ and $\mu_L^{av}=0.051\mu_B$. We note that within this approach all Fe atoms are assumed to be equivalent, since the individual moments of Fe I and Fe II are not distinguishable. Since our additional magnetization measurements of 4, 8, and 40 nm thick films show no thickness dependence of the total magnetic moment, the small difference between our theoretical and experimental results for the average spin moment is not an interfacial effect and must be attributed to small *B*2 domains which have $\mu_S^{av}\approx 0$ and were observed in our samples by XRD.

For additional justification of the effect of Fe-Si hybridization on the magnetic moments, we experimentally studied the case when a Si (an Fe) atom is replaced by an Fe (a Si) atom in the unit cell. This roughly corresponds to an increase or decrease of the Fe and Si concentrations in Fe_3Si alloy by $\pm 5\%$. The unit cell of $Fe_{3.2}Si_{0.8}$ consists of about 13 Fe atoms (5 bcc and 3 *B*2 sublattices); the one of $Fe_{2.8}Si_{1.2}$ consists of about 12 Fe atoms (3 bcc and 5 *B*2 sublattices). These replacements modify the number of Fe–Si bonds and consequently change the average Fe moment. The experimental results for these off-stoichiometric samples are summarized in the lower part of Table I.

Both the spin and orbital moments increase as the Fe concentration increases (Table I), confirming that replacing one Si atom with Fe reduces the effective Fe-Si hybridization in the system and enhances the average atomic moment. A reversed mechanism takes place when one Fe atom is replaced by Si which accordingly explains the decreased average Fe moments in $Fe_{2.8}Si_{1.2}$. Interestingly, the orbital moment increases faster than the spin moment for a smaller Si concentration, which indicates that in addition to the spin-orbit splitting, the ligand field plays an important role in the unquenching of the orbital moment.

V. SUMMARY

In summary, we compared experimentally determined spin and orbital moments in Fe_3Si with the ones determined by DFT based calculations. We found good agreement and show that the Fe-Si hybridization increases the ligand field on Fe sites and consequently modifies the orbital quenching in $Fe_{3\pm\delta}Si_{1\mp\delta}$ binary Heusler alloys. Furthermore, we have found that both spin and orbital moments can be tuned within a wide range by slightly modifying the stoichiometry. Thus, our results may be of importance for controlling magnetic properties in ferromagnet and/or semiconductor interface in novel spintronic devices where the efficiency of the device depends on the local properties of the magnetic moment.

ACKNOWLEDGMENTS

The authors would like to thank W. Keune, U. K. Utochkina, U. von Hörsten, and H. Wende for sample preparation and valuable discussion. This work has been supported by the Deutsche Forschungsgemeinschaft, Sfb 491. S.J.H. acknowledges support by the Alexander-von-Humboldt Foundation.

*zakeri@agfarle.uni-duisburg.de; Present address: Max-Planck Institute of Microstructure Physics, Weinberg 2, D-06120 Halle, Germany, zakeri@mpi-halle.de

†Present address: Department of Physics, Isfahan University of Technology, 84156 Isfahan, Iran.

[1] H. J. Elmers, G. H. Fecher, D. Valdaitsev, S. A. Nepijko, A. Gloskovskii, G. Jakob, G. Schonhense, S. Wurmehl, T. Block, C. Felser, P.-C. Hsu, W.-L. Tsai, and S. Cramm, Phys. Rev. B **67**, 104412 (2003).

[2] H. J. Elmers, S. Wurmehl, G. H. Fecher, G. Jakob, C. Felser, and G. Schönhense, Appl. Phys. A: Mater. Sci. Process. **79**, 557 (2004).

[3] H. J. Elmers, S. Wurmehl, G. H. Fecher, G. Jakob, C. Felser, and G. Schönhense, J. Magn. Magn. Mater. **272**, 758 (2004).

[4] S. Wurmehl, G. H. Fecher, K. Kroth, F. Kronast, H. A. Dürr, Y. Takeda, Y. Saitoh, K. Kobayashi, H. Lin, G. Schönhense, and C. Felser, J. Phys. D **39**, 803 (2006).

[5] S. Wurmehl, G. H. Fecher, H. C. Kandpal, V. Ksenofontov, C. Felser, H. J. Lin, and J. Morais, Phys. Rev. B **72**, 184434 (2005).

[6] K. Miyamoto, A. Kimura, K. Iori, K. Sakamoto, T. Xie, T. Moko, S. Qiao, M. Taniguchi, and K. Tsuchiya, J. Phys.: Condens. Matter **16**, S5797 (2004).

[7] R. Kelekar, H. Ohldag, and B. M. Clemens, Phys. Rev. B **75**, 014429 (2007).

[8] M. Sargolzaei, M. Richter, K. Koepernik, I. Opahle, H. Eschrig, and I. Chaplygin, Phys. Rev. B **74**, 224410 (2006).

[9] S. Picozzi, A. Continenza, and A. J. Freeman, Phys. Rev. B **66**, 094421 (2002).

[10] I. Galanakis, Phys. Rev. B **71**, 012413 (2005).

[11] S. H. Liou, S. S. Malhotra, J. X. Shen, M. Hong, J. Kwo, H. S. Chen, and J. P. Mannaerts, J. Appl. Phys. **73**, 6766 (1993).

[12] J. Herfort, H.-P. Schönherr, and K. H. Ploog, Appl. Phys. Lett. **83**, 3912 (2003); J. Herfort, H.-P. Schönherr, K.-J. Friedland, and K. H. Ploog, J. Vac. Sci. Technol. B **22**, 2073 (2004); J. Herfort, H.-P. Schönherr, A. Kawaharazuka, M. Ramsteiner, and K. H. Ploog, J. Cryst. Growth **278**, 666 (2005).

[13] N. Onda, H. Sirringhaus, S. Goncalves-Conto, C. Schwarz, S. Zehnder, and H. von Känel, Appl. Surf. Sci. **73**, 124 (1993).

[14] M. Mendik, Z. Frait, H. von Känel, and N. Onda, J. Appl. Phys. **76**, 6897 (1994).

[15] B. Jenichen, V. M. Kaganer, J. Herfort, D. K. Satapathy, H. P. Schönherr, W. Braun, and K. H. Ploog, Phys. Rev. B **72**, 075329 (2005).

[16] A. Ionescu, C. A. F. Vaz, T. Trypiniotis, C. M. Gürtler, H. García-Miquel, J. A. C. Bland, M. E. Vickers, R. M. Dalgliesh, S. Langridge, Y. Bugoslavsky, Y. Miyoshi, L. F. Cohen, and K. R. A. Ziebeck, Phys. Rev. B **71**, 094401 (2005); A. Ionescu, C. A.

F. Vaz, T. Trypiniotis, C. M. Gürtler, M. E. Vickers, H. García-Miquel, and J. A. C. Bland, J. Magn. Magn. Mater. **286**, 72 (2005).

[17] S. Adoh, M. Kumano, R. Kizuka, K. Ueda, A. Kenjo, and M. Miyao, Appl. Phys. Lett. **89**, 182511 (2006); R. Nakane, M. Tanaka, and S. Sugahara, *ibid.* **89**, 192503 (2006); T. Yoshitake, D. Nakagauchi, T. Ogawa, M. Itakura, N. Kuwano, Y. Tomokiyo, T. Kajiwara, and K. Nagayama, *ibid.* **86**, 262505 (2005).

[18] C. Kittel, Phys. Rev. **76**, 743 (1949); A. J. P. Meyer and G. Asch, J. Appl. Phys. **32**, S330 (1961), and references therein.

[19] Kh. Zakeri, I. Barsukov, N. K. Utochkina, F. M. Römer, J. Lindner, R. Meckenstock, U. von Hörsten, H. Wende, W. Keune, M. Farle, S. S. Kalarickal, K. Lenz, and Z. Frait, Phys. Rev. B **76**, 214421 (2007).

[20] P. Blaha, K. Schwarz, G. K. H. Madsen, D. Kvasnicka, and J. Luitz, *WIEN2k, An Augmented Plane Wave + Local Orbitals Program for Calculating Crystal Properties* (Technische Universität Wien, Vienna, Austria, 2001) (www.wien2k.at).

[21] H. Wu, P. Kratzer, and M. Scheffler, Phys. Rev. B **72**, 144425 (2005).

[22] S. Fujii, S. Ishida, and S. Asano, J. Phys. Soc. Jpn. **64**, 185 (1995).

[23] E. G. Moroni, W. Wolf, J. Hafner, and R. Podloucky, Phys. Rev. B **59**, 12860 (1999).

[24] A. Bansil, S. Kaprzyk, P. E. Mijnarends, and J. Tobola, Phys. Rev. B **60**, 13396 (1999), and references therein.

[25] N. I. Kulikov, D. Fristot, J. Hugel, and A. V. Postnikov, Phys. Rev. B **66**, 014206 (2002).

[26] S. Dennler and J. Hafner, Phys. Rev. B **73**, 174303 (2006), and references therein.

[27] V. A. Niculescu, T. J. Burch, and J. I. Budnick, J. Magn. Magn. Mater. **39**, 223 (1983).

[28] S. Blundell, *Magnetism in Condensed Matter* (Oxford University Press, New York, 2001), p. 35.

[29] S. Cottenier (private communication).

[30] H. Ebert, Rep. Prog. Phys. **59**, 1665 (1996).

[31] M. Farle, Rep. Prog. Phys. **61**, 755 (1998).

[32] Kh. Zakeri, Th. Kebe, J. Lindner, C. Antoniak, M. Farle, K. Lenz, T. Toli'nski, and K. Baberschke, Phase Transitions **79**, 793 (2006).

[33] Kh. Zakeri, J. Lindner, I. Barsukov, R. Meckenstock, M. Farle, U. von Hörsten, H. Wende, W. Keune, J. Rocker, S. S. Kalarickal, K. Lenz, W. Kuch, K. Baberschke, and Z. Frait, Phys. Rev. B **76**, 104416 (2007).

[34] J. Smit and H. G. Beljers, Philips Res. Rep. **10**, 133 (1955).

[35] A. N. Anisimov, M. Farle, P. Poulopoulos, W. Platow, K. Baberschke, P. Isberg, R. Wäppling, A. M. N. Niklasson, and O. Eriksson, Phys. Rev. Lett. **82**, 2390 (1999).

[36] J. Pelzl, R. Meckenstock, D. Spoddig, F. Schreiber, J. Pflaum, and Z. Frait, J. Phys.: Condens. Matter **15**, S451 (2003).